SPECT Imaging for Temporal Dynamics of Thyroidal and Salivary Radionuclide Accumulation in 17-AAG Treated Thyroid Cancer Mouse Model

Yu-Yu Liu

The Ohio State Biochemistry Program, The Ohio State University, Columbus, OH and Department of Physiology and Cell Biology, The Ohio State University, Columbus, OH

Abstract

Selective iodide uptake and prolonged iodine retention in the thyroid is the basis for targeted radioiodine therapy for thyroid cancer patients, however, salivary gland dysfunction is the most frequent non-thyroidal complications. In this study we employed non-invasive SPECT functional imaging to quantify the temporal dynamics of thyroidal and salivary radioiodine accumulation in mice. At 60 min post radionuclide injection, radionuclide accumulation in the salivary gland was generally higher than that in thyroid due to much larger volume of the salivary gland. However, radionuclide accumulation per anatomic unit in the salivary gland was lower than that in thyroid and was comparable among mice of different age and gender. Differently, radionuclide accumulation per anatomic unit in thyroid varied greatly among mice. The extent of thyroidal radioiodine accumulation stimulated by a single dose of exogenous bovine TSH (bTSH) in T3-supplemented mice was much less than that in mice received neither bTSH nor T3 (non-treated mice), suggesting that the duration of elevated serum TSH level is

important to maximize thyroidal radioiodine accumulation. Furthermore, the extent and duration of radioiodine accumulation stimulated by bTSH was less in the thyroids of the thyroid-targeted RET/PTC1 (Tg-PTC1) mice bearing thyroid tumors compared to the thyroids in wild type mice. Lastly, the effect of 17-AAG on increasing thyroidal, but not salivary, radioiodine accumulation was validated in both wild type mice and Tg-PTC1 preclinical thyroid cancer mouse model.

Introduction

The primary function of the thyroid gland is to synthesize thyroid hormones, thriiodothyronine (T3) and thyroxine (T4), which play important roles in systemic metabolism. Iodine is an essential component of thyroid hormone yet it is frequently not abundant in the diet; therefore the thyroid gland has evolved an effective way to sequester iodine 20 to 40 times against its concentration gradient from the systemic circulation. Iodide is transported into thyroid follicular cells by the sodium iodide symporter (NIS), an intrinsic membrane glycoprotein expressed on the basolateral membrane of the thyroid follicular cells. Once in the thyroid cells, iodine is incorporated into thyroglobulin (Tg) through a process called iodine organification and stored in the follicular lumen of the thyroid. Effective radioiodine accumulation in thyroid tissues, mediated by both active uptake and organification, has allowed the clinical use of radioiodine to detect and/or ablate residual thyroid cancer tissue in patients who have undergone thyroidectomy (see review in Shen *et al.* 2001).

Both iodide uptake and organification are mainly stimulated by thyrotropin (TSH). To selectively induce radioiodine accumulation in thyroid tissues for effective radioiodine therapy, TSH is elevated either by T4 withdrawal to induce endogenous hypothyroidism or by exogenous administration of recombinant human TSH (rhTSH) prior to radioiodine administration (see guidelines published by Copper *et al.* 2009; Luster *et al.* 2008). However, about 20-30% patients with metastatic thyroid cancer do not benefit from radioiodine therapy due to reduced or absent NIS expression/function (Caillou *et al.* 1998; Castro *et al.* 2001; Oler Et Cerutti 2009; Patel *et al.* 2002; Ward *et al.*

2003). Thus, it is of clinical importance to identify/develop pharmacological reagents that could increase and/or restore radioiodine accumulation in these tumors. As radioiodine accumulation is the net outcome of iodide influx and efflux, strategies to increase radioiodine accumulation include selectively increase thyroidal iodide influx and/or decrease iodide efflux.

Much effort has been made to identify reagents that increase NIS mRNA levels and/or radioiodine accumulation in cultured thyroid cells. DNA methylation inhibitor 5-azacytidine (Provenzano *et al.* 2007; Venkataraman *et al*. 1999) and H-DAC inhibitor depsipeptide (Kitazono *et al.* 2001) appear to modestly increase in NIS mRNA level as well as radioiodine accumulation in both thyroid and non-thyroid cancer cells. Conversely, pharmacological inhibitors of MAPK or PI3K/Akt signaling pathways were reproducibly shown to increase NIS expression/function in immortalized non-transformed cultured thyroid cells (Garcia Et Santisteban 2002; Knauf *et al.* 2003; Kogai *et al.* 2008; Vadysirisack *et al.* 2007; Zaballos *et al.* 2008). A recent study showed that combination treatment of inhibitors for H-DAC, MAPK, and PI3K increased radioiodine accumulation in several human thyroid cancer cell lines (Hou *et al.* 2010), but this finding is yet to be confirmed by others. Most importantly, to our knowledge, none of these findings have been validated using immune-competent genetically engineered mice carrying thyroid tumors surrounded by physiologically/pathologically relevant microenvironment.

Our lab has previously reported that 17-allyamino-17-demothoxygeldanamycin (17-AAG) increases NIS-mediated radioiodine accumulation by decreasing iodide efflux in NIS-expressing PC Cl3 rat thyroid cells and PC Cl3 cells stably expressing RET/PTC1

(Marsee *et al.* 2004). This finding was subsequently confirmed by another study showing that 17-AAG increases iodide retention in cultured human anaplastic thyroid cancer cells stably expressing hNIS (Elisei *et al.* 2006). In our current study, we used non-invasive radionuclide imaging with micro-single photon emission computed tomography (micro-SPECT) to validate the effect of 17-AAG on increasing thyroidal, but not salivary, radioiodine accumulation in wild type (WT) mice and in our thyroid-targeted RET/PTC1 (Tg-PTC1) thyroid cancer mouse model. Our findings encourage the investigation of 17-AAG derivative pharmacological agents to increase the efficacy of radioiodine therapy in thyroid cancer patients, in addition to their potential roles as novel chemotherapeutic agents.

Material and Methods

Animals and Treatment

The study protocol (2009A0118) was approved by our Institutional Animal Care and Use Committee that oversees the responsible use of animals in university research and instructional activities. All research activities were conformed to the statutes of the Animal Welfare Act and the guidelines of the Public Health Service as issued in the Guide for the Care and Use of Laboratory Animals (revised 1996). Tg-PTC1 mice were generated in the FVB/N background, and all Tg-PTC1 mice developed thyroid tumors by one month of age (Cho *et al.* 1999; Jhiang *et al.* 1996). For T3-bTSH experiments, mice were supplemented with 12 μg/ml T3 in their drinking water daily. On day 5, mice received a single intraperitoneal (i.p.) injection of bTSH in 200 μl 1% BSA/PBS and after 16 hr the mice were subjected to SPECT imaging, or sacrificed for *ex vivo* gamma counting, as described below. The bTSH dosages utilized are reported at the result section.

Two different experimental plans were employed for 17-AAG (National Cancer Institute: NCI 330507) experiments. We started with the protocol of using T3-bTSH treated mice i.p. injected with a single dose of 40 mg/kg 17-AAG (the highest dose used in mice reported in NCI Investigator brochure, 2004) and performed SPECT imaging at 2 hr post 17-AAG injection. We later modified the protocol using mice neither treated with T3 nor bTSH (non-treated mice) i.p. injected with a single dose of 30 mg/kg 17-AAG and performed SPECT imaging at 3 hr post 17-AAG injection.

In vivo multi-pinhole SPECT imaging

Small animal SPECT imaging was performed using the X-SPECT preclinical platform (Gamma Medica, CA, USA) equipped with 2 gamma cameras, each mounted with a multiple pinhole collimator with 1 mm aperture. After i.p. injection of 100-150 μCi $Na^{123}I$ ($t_{1/2}$= 13.3 hr) or $Na^{99m}TcO_4$ ($t_{1/2}$= 6.01 hr) in saline, mice were anesthetized using isofluorane inhalation and immobilized on the animal bed. For subsequent calibration of radioactivity in target tissues at various times, a 0.25 ml eppendorf tube containing a known amount of the same radionuclide was included as a decay control (DC). SPECT imaging was acquired with 32 projections, each for 50 sec on a 30 mm radius of rotation. SPECT images were acquired at 1, 6, and 24 hr post $Na^{123}I$ injection or 1 hr post $Na^{99m}TcO_4$ injection.

Ex vivo gamma counting

Following T3-bTSH treatment, animals were i.p. injected with 20-40 μCi $Na^{123}I$ in saline. Animals were sacrificed at 6 hr post $Na^{123}I$ injection, and thyroid gland, salivary gland and liver were harvested and their radioactivity measured with a gamma counter (Perkin Elmer, MA, USA) along with a known activity of $Na^{123}I$ as a standard for quantification.

Calculation of thyroidal and salivary radioiodine accumulation

The total injected dose was calculated by subtracting the post-injected syringe counts from the pre-injected syringes counts. Using the Amira 3.1 software (Gamma Medica, CA, USA), region of interest (ROI) was manually drawn over the thyroid gland, salivary gland, or decay control on xy, yx, and xz-planes, and the total radioactivity in the 3D

region defined by the three selected planes was automatically determined. Thyroidal and salivary radioiodine accumulation were calibrated by decay control counts at each time point and reported as the percentage of injected dose (%ID).

Statistical Analysis

As many of the experiments measured thyroidal radioiodine accumulation in mice over time, linear mixed models were used to take account of the dependency of observations within the same animals. To ensure unbiased hypothesis tests, we used a covariance structure estimation method for small samples that avoids underestimation of experimental error. Two sample t-tests were used for simple two group comparisons and Holm's step down procedure (Holm 1979) was used to adjust for multiple comparisons. P-values $<.05$ for single comparisons or after adjustment for multiple comparisons were considered as significant.

Results

Temporal dynamics of radioiodine accumulation in thyroid and salivary glands evaluated by 3D SPECT functional imaging

Thyroidal iodide accumulation is largely the sum of NIS-mediated iodide uptake along with iodide retention by iodide organification. In comparison, salivary glands accumulate iodide through NIS-mediated iodide uptake but they lack iodide organification. The temporal dynamics of ^{123}I accumulation in thyroid and salivary glands in WT mice was examined by non-invasive SPECT nuclear imaging (Fig. 1). At 1 hr post Na^{123}I injection (t1), ^{123}I accumulation was evident in both thyroid and salivary glands. At 6 hr post Na^{123}I injection (t6), ^{123}I accumulated in the thyroid gland was further increased due to continued iodide uptake and organification. However, ^{123}I accumulated in the salivary gland was decreased due to lack of iodide organification and decreased ^{123}I in the blood circulation. At 24 hr post Na^{123}I injection (t24), ^{123}I accumulation in the thyroid gland continued to increase when normalized by physical decay. Conversely, no ^{123}I accumulation was detected in the salivary gland at t24, suggesting that ^{123}I was completely cleared from the blood circulation by excretion or tissue uptake in other tissues such as the thyroid. Consequently, thyroidal radioiodine accumulation at t24 was mainly contributed by iodide retention.

Several mice were subjected to SPECT imaging in the same experimental settings as stated above. The amount of ^{123}I accumulation in the thyroid (%ID) varied extensively among mice and the degree of ^{123}I accumulation at t6 was not always near maximum, i.e. to the similar extent seen at t24 (Fig. 2). Thyroidal %ID at t1, t6, and t24 for each mice

studied are shown in Table 1 (t1: 0.63-6.45%, mean= 2.07%; t6: 1.59-23.21%, mean= 8.88%; and t24: 1.48-24.66%, mean= 11.55%). Albeit our small sample number, mice of 14-15 months of age tended to have lower iodide influx as indicated by thyroidal %ID at t1. Mice of 2-3 months old appeared to have lower iodide retention ability as indicated by lower ratios of t6 or t24 over t1 thyroidal %ID. This may be at least in part contributed by their faster renal clearance rate as shown by a sharper decrease in ^{123}I accumulation in salivary gland at t6 versus t1 (t6/t1 %ID: 2-3 month: 0.1-0.3, mean= 0.22, N=3; > 6 month: 0.73-1.01, mean= 0.86, N=4). These findings warrant further study using a larger cohort.

The extent of single dose bTSH induced thyroidal radioiodine accumulation in T3-supplemented mice is less than that induced by continuous stimulation of endogenous mouse TSH in non-treated mice

To examine the effect of exogenous bTSH on temporal dynamics of thyroidal radioiodine accumulation in the absence of endogenous mouse TSH (mTSH), endogenous mTSH was suppressed by T3 supplementation in WT mice. As shown in Fig. 2, thyroidal radioiodine accumulation was diminished in all mice that underwent T3 supplementation (t1: 0.18-1.06%, mean= 0.49%; t6: 0.26-0.59%, mean= 0.41%; t24: 0-0.2%, mean= 0.06%, N=4), despite extensive variability of thyroidal radioiodine accumulation seen in non-treated mice (N=11). This data confirms that our T3 supplementation protocol is sufficient to suppress endogenous mTSH induced thyroidal radioiodine accumulation, regardless of age and gender.

In mice treated with 6, 30, or 60 μg of bTSH at day 5 of T3-supplementation, thyroidal radioiodine accumulation was increased in a dose-dependent manner (data not shown). Further increase of bTSH to 90 μg did not further increase (p-value=0.71) thyroidal radioiodine accumulation as determined by *ex vivo* gamma counting of thyroids at 6 hr post $Na^{123}I$ injection (Fig. 3A). As shown in Fig. 2, thyroidal radioiodine accumulation averaged across time was significantly increased (p-value= 0.0007) by a single dose of 60 μg bTSH in T3 supplemented mice (t1: 0.34-1.99%, mean= 0.93%; t6: 1.22-2.84%, mean= 2.01%; t24: 1.97-3.36%, mean= 2.46%, N=5). However, thyroidal %ID in T3-bTSH treated mice was much lower (p-value= 0.027) than that in non-treated mice. This is most likely due to the short half-life of bTSH (< 3hr, Guyot *et al.* 2007), such that a single dose of 60 μg bTSH in T3 supplemented mice is not sufficient to induce thyroidal radioiodine accumulation comparable to non-treated mice which had continuous low-level stimulation of endogenous mTSH.

The extent and duration of thyroidal radioiodine accumulation induced by bTSH is less in Tg-PTC1 mice than that in wild type mice

Tg-PTC1 mice can serve as a preclinical animal model to examine factors that modulate radioiodine accumulation in thyroid tumors. We previously reported that thyroidal radioiodine accumulation in Tg-PTC1 mice is decreased compared to WT mice at 6 hr post $Na^{125}I$ injection when normalized with tissue weight despite of elevated serum TSH level in Tg-PTC1 mice (Cho *et al.* 1999). This is consistent with clinical findings that malignant thyroid tumors are typically “cold” nodules. Our pilot study showed that thyroidal radioiodine accumulation was also suppressed by T3

supplementation in Tg-PTC1 mice (data not shown). To compare the responsiveness of WT and Tg-PTC1 mice to exogenous bTSH toward induction of thyroidal radioiodine accumulation, ^{123}I accumulation at t6 was evaluated in T3 supplemented mice injected with a single dose of bTSH. As shown in Fig. 3A, the extent of bTSH induced thyroidal radioiodine accumulation at t6 in Tg-PTC1 mice (1.6-2.5%, mean= 2.04%, N=4) was significantly lower (p-value= 0.001) than that in WT mice (8.9-16.3%, mean= 12.44%, N=4) without normalization for thyroid gland volume or weight. However, the size of thyroid glands in Tg-PTC1 mice was consistently larger than that in WT mice.

To compare the duration of bTSH-induced NIS activity between WT mice and Tg-PTC1 mice, $Na^{99m}TcO_4$, which cannot be organified, was used to evaluate NIS-mediated radionuclide influx at 17 hr or 41 hr post bTSH administration. As shown in Fig. 3B, thyroidal %ID of $Na^{99m}TcO_4$ was modestly decreased (p-value= 0.28) at 41 hr compared to 17 hr post bTSH administration in WT mice (17 hr: 1.27-1.54%, mean= 1.41%; 41 hr: 0.23-1.50%, mean= 0.93%, N=3). In comparison, thyroidal %ID of $Na^{99m}TcO_4$ was significantly decreased (p-value= 0.0076) at 41 hr in all three Tg-PTC1 mice examined (17 hr: 1.7-2.60%, mean= 2.01%,; 41 hr: 0.00-0.57%, mean= 0.32%, N=3). Indeed, statistical analysis by linear mixed model showed that the difference of NIS activity between 17 hr and 41 hr post bTSH administration for Tg-PTC1 mice was much more evident (p-value= 0.014) than that for WT mice. Taken together, thyroid tumor bearing thyroid glands of Tg-PTC1 mice not only were less responsive to bTSH in the induction of radioiodine accumulation; the duration of NIS induction was also much shorter than normal thyroids in WT mice. It is interesting to note that thyroidal %ID of $Na^{99m}TcO_4$ at 17 hr post bTSH injection in Tg-PTC1 mice was higher compared to WT

mice, suggesting that the number of thyroid follicular cells responsive to bTSH at an early time point in Tg-PTC1 mice is much more than that in WT mice. This phenomenon can be explained by increased proliferation of thyroid follicular cells (Cho *et al.* 1999) and the much larger size of thyroids observed in Tg-PTC1 mice.

The area under time-activity curve of thyroid in wild type mice is markedly increased by 30 mg/kg 17-AAG

None of the T3-bTSH mice injected with a single dose of 40 mg/kg 17-AAG survived during SPECT imaging acquisition (N=3, data not shown), indicating the experimental condition was not tolerable by the mice. We then examined the effect of 30 mg/kg 17-AAG in non-treated mice which had $Na^{123}I$ injection at 3 hr post 17-AAG injection (see the top panel of Fig. 4). Three experimental trials with identical design were performed to compare temporal radioiodine accumulation between DMSO and 17-AAG treated mice. As shown in Fig 4, thyroidal radioiodine accumulation at t24 in 17-AAG treated mice was much higher (p-value= 0.15) than DMSO-treated mice in each experimental trial (DMSO vs. 17-AAG: 5.42% vs. 9.22%; 20.66% vs. 65.88%; 8.07% vs. 55.05%), despite extensive variations of thyroidal %ID among different experimental trials. Conversely, thyroidal radioiodine accumulation at t1 was not increased (p-value= 0.98) by 17-AAG treatment (DMSO vs. 17-AAG: 3.58% vs. 4.02%; 1.18% vs. 0.63%; 3.24% vs. 3.44%). These results indicate that 17-AAG markedly increases iodide retention although it has little effect on NIS-mediated iodide influx.

The average of thyroidal %ID at t1, t6, and t24 among three experimental trials as well as the average ratio of thyroidal %ID at t6 or t24 versus t1 in each experimental trial

are shown in Table 2. Iodide retention ability in WT mice was moderately increased by 17-AAG at t6 (~ 2 fold), and further increased at t24 (~ 4 fold) as compared to DMSO treated mice. Consequently, the exposure of the thyroid to radioiodine over time was markedly increased by 17-AAG as defined by the area under time-activity curve (AUC). Indeed, while the value of AUC varied greatly among experimental trials (DMSO: 224.4 ± 133.2, N=3; 17-AAG: 583.1 ± 362.1, N=3), the fold increase in AUC by 17-AAG calculated in each experimental trial ranged from 1.55 to 3.96. Taken together, the effect of 17-AAG on increasing radioiodine accumulation in cultured thyroid cells is validated in WT mice using temporal SPECT imaging. Furthermore, 17-AAG did not appear to have a effect on salivary %ID (data not shown).

The area under time-activity curve of thyroid tumor in Tg-PTC1 mice is markedly increased by 30 mg/kg 17-AAG

We next examined the effect of 30 mg/kg 17-AAG on thyroidal radioiodine accumulation in thyroid tumor bearing thyroid glands of Tg-PTC1 mice. While WT mice were tolerant of 30mg/kg 17-AAG treatment, two out of four Tg-PTC1 mice did not survive through SPECT imaging acquisition. However, as shown in Fig. 5, both of the remaining Tg-PTC1 mice treated with 17-AAG had evident increase of thyroidal radioiodine accumulation compared to mice treated with DMSO at t24 (DMSO vs. 17-AAG: 3.50% vs. 25.89%; 2.53% vs. 19.23%). Similar to WT mice, 17-AAG appeared to increase radioiodine retention rather than radioiodide influx in Tg-PTC1 mice. As shown in Table 2, iodide retention was moderately increased by 17-AAG at t6 (~ 1.5 fold), yet it was further increased at t24 (~ 4 fold) as calculated by the average ratios of

thyroidal %ID at t6 or t24 versus t1 in each experimental trial. The value of AUC was less variable between the two experimental trials in Tg-PTC1 mice (DMSO: 148.8 ± 44.3, N=2; 17-AAG: 442.6 ± 62.7, N=2), and the fold increase in AUC by 17-AAG in the two experimental trials were 2.21 and 4.14. Thyroidal iodide retention ability in 17-AAG treated Tg-PTC1 mice (t24/t1 %ID= 2.6 ± 0.6) was much lower than that in WT mice (t24/t1 %ID= 15.7 ± 0.9) at t24, yet the fold increase of iodide retention ability by 17-AAG was comparable between Tg-PTC1 mice and WT mice at t24. Taken together, the effect of 17-AAG on increasing thyroidal radioiodine accumulation is confirmed in a preclinical thyroid cancer animal model.

Discussion

In this study, we quantified temporal radioiodine accumulation in both thyroid and salivary glands modulated by T3, bTSH and/or 17-AAG in mice using SPECT functional imaging. By comparing temporal dynamics of radioiodine accumulation between salivary and thyroid glands, we found that administered radioiodine was almost completely cleared from blood circulation after 24 hr, and that iodide organification contributes greatly to thyroidal radioiodine accumulation over time. The extent of thyroidal radioiodine accumulation stimulated by a single dose of exogenous bTSH in T3 supplemented mice was much less than that in non-treated mice, justifying the clinical use of multiple doses of rhTSH or the merit of T4 withdrawal in thyroid cancer patients prior to radioiodine therapy. Furthermore, the extent and duration of radioiodine accumulation stimulated by bTSH was reduced in thyroid tumor bearing thyroid glands of Tg-PTC1 mice compared to the thyroids in WT mice. Lastly, 17-AAG significantly increased thyroidal exposure of radioiodine over time in our Tg-PTC1 preclinical thyroid cancer mouse model, which encourages the study of 17-AAG derivatives not only as novel chemotherapeutic agents to impede tumor progression but also to improve radioiodine therapy in patients with thyroid cancer. Optimally, 17-AAG derivatives could permit those tumors with low radioiodine accumulation to become amenable to radioiodine treatment and allow for those tumors with normal radioiodine accumulation to be affectively treated with lower radioiodine activities.

Salivary gland dysfunction is the most frequent non-thyroidal complications of radioiodine therapy for patients with thyroid cancer (Kloos 2009). A better understanding

of the temporal dynamics of radioiodine accumulation in the thyroid and salivary glands may lead to strategies to mitigate radioiodine-induced salivary gland damage without compromising the efficacy of thyroid cancer radioiodine therapy. A recent study showed that the time required to reach maximal accumulation of $^{99m}TcO_4$ uptake in thyroid glands is shorter than that in salivary glands of C57 BL6/6J mice (Franken *et al.* 2010). This difference could be explained by higher NIS transport activity and/or smaller NIS-expressing epithelial cell-delimiting compartments of the thyroid, i.e. thyroid colloid versus salivary acini and duct lumens. Similarly, the rate of decrease in $^{99m}TcO_4$ accumulation is faster in the thyroid than in the salivary gland after administration of competitive inhibitors (Franken *et al.* 2010). In the current study, we showed that salivary gland %ID was 1.02-5.75 fold higher than thyroid %ID at t1 (see Table 1), which has been reported by others (Franken *et al.* 2010; Zuckier *et al.* 2004) and is anticipated by the larger size of the salivary gland. Indeed, voxel counts in the selected ROI of salivary were 1.93-9.38 fold higher than those of the thyroid at t1 (data not shown), although functional voxel counts in selected ROI may not exactly reflect anatomic volume of the target tissue. Interestingly, the normalized means (total signal intensity counts divided by voxel counts) of salivary glands at t1 were lower than those of the thyroids (salivary/thyroid= 0.47-0.94 with a mean of 0.68), indicating that NIS expression/activity per anatomic unit is lower in salivary gland compared to the thyroid gland. Salivary normalized means at t1 were quite comparable among mice (62-80 with a mean of 72), yet thyroid normalized means at t1 varied greatly among mice (66-163 with a mean of 113). Thus, NIS activity per anatomic unit in the salivary gland does not appear to be modulated by gender or age among different mice.

It is of interest to note that the ratio of salivary %ID versus thyroidal %ID at t1 appeared to be greater in male (1.84-4.63, mean= 3.47, N=3) than in female (1.02-2.29, mean= 1.59, N=3) mice and seemed to increase with age (2-3 month: 1.02-3.95, mean= 2.07, N=4; 6-7 month: 2.29-4.63, mean= 3.46, N=2; 14-15 month: 5.11-5.75, mean= 5.43, N=2). This finding is consistent with the reports that total accumulation of ^{131}I uptake in submaxillary glands is greater in male than in females in several strains of mice (Llach *et al.* 1960). The reasons underlying the increase of salivary/thyroid %ID ratio with age is unknown as the variations of salivary %ID or thyroid %ID did not correlate with age. If the dependence of the ratio of salivary %ID versus thyroidal %ID at t1 on gender and age holds true in humans, and if salivary gland damage occurs at an early stage of ^{131}I exposure, we would anticipate that male and elder patients would experience more salivary dysfunction after radioiodine therapy. Finally, ^{123}I accumulation was not detectable in the salivary gland at t24 in all mice of 2-20 months old. This is consistent with the report that radioiodine in blood circulation was completely excreted by 19 hr post Na^{125}I injection in CD1 mice (Zuckier *et al.* 2004).

It has been shown that normal women had slightly higher thyroidal uptake than men at both 2 hr and 24 hr post ^{131}I administration. Furthermore, thyroidal uptake decreased slightly when subjects were aged more than 40 years old compared to those younger than 40 years at both 2 hr and 24 hr post ^{131}I administration (González E *et al.* 2008). In another study, thyroidal uptake was shown to increase with age to a maximum at about 40 years old, then decreased afterwards at both 4 hr and 24 hr post ^{131}I administration (Schober *et al.* 1976). Despite our small sample number, we did observe that female mice had higher thyroidal radioiodine accumulation compared to that of male

mice at t1 (female: 0.63-6.45%, mean= 2.74%; male: 0.90-2.94%, mean= 1.77%), t6 (female: 1.59-23.21%, mean= 11.39%; male: 2.85-18.45%, mean= 6.79%) and t24 (female: 1.48-24.66%, mean= 13.27%; male: 3.62-21.26%, mean= 10.41%). Taken together, it would be interesting to investigate whether the minimal radioactivity needed to ablate thyroid remnant in low-risk patients could be stratified by gender and age based on their differences in the magnitude of thyroidal radioiodine accumulation.

While rhTSH administration has been shown to be equally effective compared to thyroid hormone withdrawal in preparation of low-risk patients for post-operative thyroid remnant ablation (Chianelli *et al.* 2009; Elisei *et al*. 2009; Pacini *et al.* 2006; Tuttle *et al*. 2010), it remains uncertain whether rhTSH is equally effective in treating high-risk patients with known residual cancer. The level and duration of serum TSH levels required for effective ablation of thyroid remnant could be very different from that for residual cancer and may vary depending on various somatic tumor mutations that affect radioiodine accumulation. Indeed, Potzi and colleagues reported that a higher radioactivity of ^{131}I is required to achieve comparable radioiodine accumulation in thyroid cancer metastases in patients administered radioiodine after rhTSH versus thyroid hormone withdrawal preparation (Potzi *et al.* 2006). Our current study showed that thyroidal radioiodine accumulation in T3-bTSH mice was much lower than that in non-treated mice suggesting that the duration of exposure to TSH is important to promote desirable thyroidal radioiodine accumulation. We also showed that thyroid tumor bearing thyroid glands in Tg-PTC1 mice were less responsive to bTSH induced thyroidal radioiodine accumulation than normal thyroids in WT mice. Taken together, thyroid cancer foci may require higher ^{131}I activity for treatment as opposed to normal thyroid

remnants and longer duration of elevated TSH level may be required to achieve the desirable ^{131}I activity in thyroid cancer foci. Accordingly, thyroid cancer mouse models can be invaluable to examine the concepts of magnitude and duration of serum TSH elevation required to confer sufficient radioiodine accumulation in thyroid tumors.

Findings using cultured cells do not always translate into preclinical animal models or patients. For example, leptin decreases radioiodine uptake activity in FRTL-5 immortalized rat thyroid cells (Isozaki *et al.* 2004) and rat thyroid slices (de Oliveira *et al.* 2007), yet it increases thyroidal radioiodine uptake activity in live rats (de Oliveira *et al.* 2007). The discordance is most likely explained by tissue microenvironments and/or systemic effects that do not exist in isolated cultured cell system. In this study, we confirmed that 17-AAG increases thyroid exposure to radioiodine over time in WT mice as well as Tg-PTC1 transgenic mice carrying thyroid tumors. The fact that 17-AAG did not increase thyroidal radioiodine accumulation at t1, but did at t6 and t24, indicates that 17-AAG has little effect on NIS-mediated radioiodine influx but mainly acts on iodide retention/organification. This result is consistent with our previous finding that 17-AAG increases radioiodine accumulation by decreasing iodide efflux in cultured cells (Marsee *et al.* 2004). Nevertheless, before this finding can be translated into clinical trials, a few important issues need to be addressed. Are there any differences in the effects of Hsp90 inhibitors on thyroid tumors derived from various genetic abnormalities, such as B-RAF^{V600E} mutation? Do all Hsp90 inhibitors increase thyroidal radioiodine accumulation? Which Hsp90 inhibitor has the desired pharmacokinetic and pharmacodynamic profiles? What is the optimal dose, duration, and timing of Hsp90 inhibitor treatment to increase the efficacy of radioiodine therapy? Is the magnitude of

increased radioiodine accumulation by Hsp90 inhibitors sufficient to meaningfully improve the efficacy of radioiodine therapy? Finally, while not immediately needed for Hsp90 inhibitor clinical application, what are the molecular targets of this treatment in thyroid tumors, and can they be more optimally modulated by other approaches?

Acknowledgements

We wish to thank Dr. Mitch Phelps and Dr. Jeffrey S Johnston for sharing their expertise and experience in the study of 17-AAG. We would also like to thank Dr. Xiaoli Zhang for performing the statistical analysis. This work was supported in part by National Institutes of Health grant P01CA124570 (project 3 leader: SMJ) and R01 EB001876 (to SMJ). The authors declare that there is no conflict of interest that would prejudice the impartiality of this scientific work.

References

Caillou B, Troalen F, Baudin E, Talbot M, Filetti S, Schlumberger M Et Bidart JM 1998 Na+/I- symporter distribution in human thyroid tissues: an immunohistochemical study. *The Journal of Clinical Endocrinology & Metabolism* **83** 4102-4106

Castro MR, Bergert ER, Goellner JR, Hay ID Et Morris JC 2001 Immunohistochemical analysis of sodium iodide symporter expression in metastatic differentiated thyroid cancer: correlation with radioiodine uptake. *The Journal of Clinical Endocrinology & Metabolism* **86** 5627-5632

Chianelli M, Todino V, Graziano FM, Panunzi C, Pace D, Guglielmi R, Signore A Et Papini E 2009 Low-activity (2.0 GBq; 54 mCi) radioiodine post-surgical remnant ablation in thyroid cancer: comparison between hormone withdrawal and use of rhTSH in low-risk patients. *European Journal of Endocrinology/European Federation of Endocrine Societies* **160** 431-436

Cho JY, Sagartz JE, Capen CC, Mazzaferri EL Et Jhiang SM 1999 Early cellular abnormalities induced by *RET/PTC1* oncogene in thyroid-targeted transgenic mice. *Oncogene* **18** 3659-3665

Cooper DS, Doherty GM, Haugen BR, Kloos RT, Lee SL, Mandel SJ, Mazzaferri EL, McIver B, Pacini F, Schlumberger M *et al.* 2009 Revised American Thyroid Association management guidelines for patients with thyroid nodules and differentiated thyroid cancer. *Thyroid* **19** 1167-1214

Elisei R, Vivaldi A, Ciampi R, Faviana P, Basolo F, Santini F, Traino C, Pacini F Et Pinchera A 2006 Treatment with drugs able to reduce iodine efflux significantly increases the intracellular retention time in thyroid cancer cells stably transfected with sodium iodide symporter complementary deoxyribonucleic acid. *The Journal of Clinical Endocrinology & Metabolism* **91** 2389-2395

Elisei R, Schlumberger M, Driedger A, Reiners C, Kloos RT, Sherman SI, Haugen B, Corone C, Molinaro E, Grasso L *et al.* 2009 Follow-up of low-risk differentiated thyroid cancer patients who underwent radioiodine ablation of postsurgical thyroid remnants after either recombinant human thyrotropin or thyroid hormone withdrawal. *The Journal of Clinical Endocrinology & Metabolism* **94** 4171-4179

Franken PR, Guglielmi J, Vanhove C, Koulibaly M, Defrise M, Darcourt J, Pourcher T 2010 Distribution and dynamics of (99m)Tc-pertechnetate uptake in the thyroid and other organs assessed by single-photon emission computed tomography in living mice. *Thyroid* **20** 519-526

Garcia B Et Santisteban P 2002 PI3K is involved in the IGF-1 inhibition of TSH-induced sodium/iodide symporter gene expression. *Molecular Endocrinology* **16** 342-352

González PE, Carmona ARC, Araya AVQ, Miranda KF, Massardo TV, Jiménez BR, Jaimovich RF, Gatica HR 2008 Normal 131iodine uptake values at 2 and 24 hours. *Revista Medica De Chile* **136** 1288-1293

Guyot H, Sulon J, Beckers J-F, Closset J, Lebreton P, de Oliveira LA Et Rollin F 2007 Development and validation of a radioimmunoassay for thyrotropin in cattle. *Journal of Veterinary Diagnostic Investigation* **19** 643-651

Holm S 1979 A simple sequentially rejective multiple test procedure. *Scandinavian Journal of Statistics* **6** 65-70

Hou P, Bojdani E Et Xing M 2010 Induction of thyroid gene expression and radioiodine uptake in thyroid cancer cells by targeting major signaling pathways. *The Journal of Clinical Endocrinology & Metabolism* **95** 820-828

Isozaki O, Tsushima T, Nozoe Y, Miyakawa M, Takano K 2004 Leptin regulation of the thyroids: negative regulation on thyroid hormone levels in euthyroid subjects and inhibitory effects on iodide uptake and Na+/I- symporter mRNA expression in rat FRTL-5 cells. *Endocrine Journal* **51** 415-423

Jhiang SM, Sagartz JE, Tong Q, Parker-Thornburg J, Capen CC, Cho JY, Xing S Et Ledent C 1996 Targeted expression of the ret/PTC1 oncogene induces papillary thyroid carcinomas. *Endocrinology* **137** 375-378

Kitazono M, Robey R, Zhan Z, Sarlis NJ, Skarulis MC, Aikou T, Bates S Et Fojo T 2001 Low concentrations of the histone deacetylase inhibitor, depsipeptide (FR901228), increase expression of the Na^+/I^- symporter and iodine accumulation on poorly differentiated thyroid carcinoma cells. *The Journal of Clinical Endocrinology & Metabolism* **86** 3430-3435

Kloos RT 2009 Protecting thyroid cancer patients from untoward effects of radioactive iodine treatment. *Thyroid* **19** 925-928

Knauf JA, Kuroda H, Basu S Et Fagin JA 2003 RET/PTC-induced dedifferentiation of thyroid cells is mediated through Y1062 signaling through SHC-RAS-MAP kinase. *Oncogene* **22** 4406-4412

Kogai T, Sajid-Crockett S, Newmarch LS, Liu YY Et Brent GA 2008 Phosphoinositide-3-kinase inhibition induces sodium/iodide symporter expression in rat thyroid cells and human papillary thyroid cancer cells. *The Journal of Endocrinology* **199** 243-252

Llach JL, Tramezzani JH Et Cordero F Jr. 1960 A sexual difference in the concentration of iodine-131 by the submaxillary gland of mice. *Nature* **188** 1204-1205

Luster M, Clarke SE, Ditelein M, Lassman M, Lind P, Oyen WJG, Tennvall J Et Bombardieri 2008 Guidelines for radioiodine therapy of differentiated thyroid cancer. *European Journal of Nuclear Medicine and Molecular Imaging* **35** 1941- 1959

Marsee DK, Venkateswaran A, Tao H, Vadysirisack D, Zhang Z, Vandre DD Et Jhiang SM 2004 Inhibition of heat shock protein 90, a novel RET/PTC1-associated protein, increases radioiodide accumulation in thyroid cells. *The Journal of Biological Chemistry* **279** 43990-43997

Oler G Et Cerutti JM 2009 High prevalence of BRAF mutation in a Brazilian cohort of patients with sporadic papillary thyroid carcinomas: correlation with more aggressive phenotype and decreased expression of iodide-metabolizing genes. *Cancer* **115** 972-980

de Oliveira E, Teixeira Silva Fagundes A, Teixeira Bonomo I, Curty FH, Fonseca Passos MC, de Moura EG Et Lisboa PC 2007 Acute and chronic leptin effect upon in vivo and in vitro rat thyroid iodide uptake. *Life Sciences* **81** 1241-1246

Pacini F, Ladenson PW, Schlumberger M, Driedger A, Luster M, Kloos RT, Sherman S, Haugen B, Corone C, Molinaro E *et al.* 2006 Radioiodine ablation of thyroid remnants after preparation with recombinant human thyrotropin in differentiated thyroid carcinoma: results of an international, randomized, controlled study. *The Journal of Clinical Endocrinology & Metabolism* **91** 926-932

Patel A, Jhiang S, Dogra S, Terrell R, Powers PA, Fenton C, Dinauer CA, Tuttle RM Et Francis GL 2002 Differentiated thyroid carcinoma that express sodium-iodide symporter have a lower risk of recurrence for children and adolescents. *Pediatric Research* **52** 737-744

Pötzi C, Moameni A, Karanikas G, Preitfellner J, Becherer A, Pirich C Et Dudczak R 2006 Comparison of iodine uptake in tumour and nontumour tissue under thyroid hormone deprivation and with recombinant human thyrotropin in thyroid cancer patients. *Clinical Endocrinology* **65** 519-523

Provenzano MJ, Fitzgerald MP, Krager K, Domann FE 2007 Increased iodine uptake in thyroid carcinoma after treatment with sodium butyrate and decitabine (5-Aza-dC). *Otolaryngoly Head and Neck Surgery* **137** 722-728

Schober B Et Hunt JA 1976 Evaluation of the normal range of values for uptake of radioactive iodine by the thyroid gland. *Canadian Medical Associated Journal* **115** 29-35

Shen DH, Kloos RT, Mazzaferri EL, Jhiang SM 2001 Sodium iodide symporter in health and disease. *Thyroid* **11** 415-425

Tuttle RM, Lopez N, Leboeuf R, Minkowitz SM, Grewal R, Brokhin M, Omry G Et Larson S 2010 Radioactive iodine administered for thyroid remnant ablation following recombinant human thyroid stimulating hormone preparation also has an important adjuvant therapy function. *Thyroid* **20** 257-263

Vadysirisack DD, Venkateswaran A, Zhang Z Et Jhiang SM 2007 MEK signaling modulates sodium iodide symporter at multiple levels and in a paradoxical manner. *Endocrine-Related Cancer* **14** 421-432

Venkataraman GM, Yatin M, Marcinek R Et Ain KB 1999 Restoration of iodide uptake in dedifferentiated thyroid carcinoma: relationship to human Na^+/I^- symporter gene methylation status. *The Journal of Clinical Endocrinology & Metabolism* **84** 2449-2457

Zaballos MA, Garcia B Et Santisteban P 2008 Gβγ Dimers released in response to thyrotropin activate phosphoinositide 3-kinase and regulate gene expression in thyroid cells. *Molecular Endocrinology* **22** 1183-1199

Zuckier LS, Dohan O, Li Y, Chang CJ, Carrasco N Et Dadachova E 2004 Kinetics of perrhenate uptake and comparative biodistribution of perrhenate, pertechnetate, and iodide by NaI symporter-expressing tissues in vivo. *Journal of Nuclear Medicine* **45** 500-507

Ward LS, Santarosa PL, Granja F, da Assumpção LV, Savoldi M Et Goldman GH 2003 Low expression of sodium iodide symporter identifies aggressive thyroid tumors. *Cancer Letters* **200** 85-91

Figure Legend

Figure 1. Temporal dynamics of thyroidal and salivary radioiodine accumulation in wild type mouse. A 7 month old male wild type mouse was injected with ~150 μCi $Na^{123}I$ and subjected to SPECT imaging at 1(t1), 6(t6) and 24 hr(t24) post $Na^{123}I$ injection. At t1, thyroidal radioiodine accumulation was mainly contributed by NIS-mediated ^{123}I influx from blood circulation. At t6, thyroidal radioiodine accumulation was contributed by continuous ^{123}I influx as well as ^{123}I organification/retention. At t24, thyroidal radioiodine accumulation was mainly contributed by ^{123}I organification/retention as NIS-mediated ^{123}I uptake from blood circulation in the salivary gland was observed at t1 and t6, but not at t24. Thy: thyroidal functional image; Sal: salivary functional image; DC: decay control functional image. Decay control serves to normalize counts of thyroidal radioiodine accumulation at each time-point for quantification purposes. The color bar indicates radioiodine signal intensity increases from 20 (black) to 500 (red) in arbitrary units.

Figure 2. The extent of induced thyroidal radioiodine accumulation by one dose of 60 μg bTSH in T3 supplemented mice is much less than that induced by continuous endogenous mTSH in non-treated mice. WT mice were given 12 μg/ml T3 in drinking water daily. On day 5, mice were injected with one dose of 60 μg bTSH (T3-60 μg bTSH; N=5). $Na^{123}I$ (100-150 μCi) was administered into mice at 16 hr post bTSH injection. SPECT images were taken at 1(t1), 6(t6) and 24 hr(t24) post $Na^{123}I$ injection. For comparison, T3 mice (N=4) and non-treated mice (N=11) were subjected to SPECT

imaging as well. In T3 mice, thyroidal radioiodine accumulation was almost undetected (p-value= 0.0017), confirming that T3 supplementation for 5 consecutive days is sufficient to suppress endogenous TSH induced thyroidal radioiodine accumulation. While one dose of 60 μg bTSH was sufficient to induce some extent of thyroidal radioiodine accumulation, the extent of 60 μg bTSH induced radioiodine accumulation was far less (p-value= 0.027) than that of non-treated mice.

Figure 3. The extent of thyroidal radioiodine accumulation and temporal duration of NIS-mediated thyroidal $Na^{99m}TcO_4$ influx activity induced by bTSH is less in Tg-PTC1 mice than that in wild type mice. (**A**) 7 month old WT and 4 month old Tg-PTC1 mice were given 12 μg/ml T3 in drinking water daily. On day 5, mice were injected with either one dose of 60 or 90 μg bTSH. $Na^{123}I$ (20-40 μCi) was injected into mice at 16 hr post bTSH injection. At 6 hr(t6) post $Na^{123}I$ injection, mice were euthanized and thyroids were harvested and subjected for counting of activity by a gamma counter. Statistical analysis showed that WT mice had significantly higher (p-value= 0.001) thyroidal radioiodine accumulation at t6 than Tg-PTC1 mice, while there was no significant difference (p-value= 0.71) between 60 or 90 μg bTSH induced thyroidal radioiodine accumulation in both WT and Tg-PTC1 mice. (**B**) T3-supplemented WT and Tg-PTC1 mice were administered with one dose of 60 μg bTSH. $Na^{99m}TcO_4$ (100 μCi), a substrate of NIS yet could not be organified by thyroid, was first injected into mice 16 hr post bTSH injection and SPECT images were acquired at 1 hr post $Na^{99m}TcO_4$ injection, i.e. at 17 hr post bTSH injection. A second dose of $Na^{99m}TcO_4$ (100 μCi) was injected into mice 40 hr post bTSH injection and SPECT images were acquired at 1 hr post the second

$Na^{99m}TcO_4$ injection, i.e. at 41 hr post bTSH injection. Two out of three WT mice had comparable NIS-mediated $^{99m}TcO_4$ influx activity at the two different time points, whereas all three Tg-PTC1 mice had decreased NIS-mediated $^{99m}TcO_4$ influx activity at later time point. The difference in duration of NIS-mediated thyroidal $^{99m}TcO_4$ influx activity induced by single dose of bTSH between Tg-PTC1 mice and WT mice was statistically significant (p-value= 0.014).

Figure 4. The area under time-activity curve (AUC) of thyroid in wild type mice is markedly increased by 30 mg/kg 17-AAG. WT mice (15-18 months) were weighed and injected with 30 mg/kg 17-AAG in 50 μl DMSO. $Na^{123}I$ (100-150 μCi) was injected into mice at 3 hr post 17-AAG injection. SPECT images were acquired at t1(4), t6(9) and t24(27) post $Na^{123}I$ injection (time post 17-AAG injection). At t1, the extent of thyroidal radioiodine accumulation was quite comparable between DMSO versus 17-AAG treated mice suggesting that 17-AAG had minimal effect on thyroidal iodide influx. However, at t24, the extent of thyroidal radioiodine accumulation was markedly increased (p-value= 0.15) in 17-AAG treated mice versus that in DMSO treated mice, suggesting that 17-AAG increases iodide retention ability. Consequently, the exposure of thyroid with radioiodine over time was markedly increased by 17-AAG as defined by the AUC.

Figure 5. The area under time-activity curve (AUC) of thyroid tumor in Tg-PTC1 mice is markedly increased by 30 mg/kg 17-AAG. Tg-PTC1 mice (15-21 months) were weighed and injected with 30 mg/kg 17-AAG in 50 μl DMSO. $Na^{123}I$ (100-150 μCi) was injected into mice at 3 hr post 17-AAG injection. SPECT images were acquired at t1(4),

t6(9) and t24(27) post $Na^{123}I$ injection (time post 17-AAG injection). At t24, the difference in the extent of increased thyroidal radioiodine accumulation was evidently enhanced in 17-AAG treated mice compared to that in DMSO treated mice at least in part due to the decreased thyroidal %ID by DMSO at t24 in Tg-PTC1 mice. As a result, AUC was evidently increased by 17-AAG in Tg-PTC1 mice.

Figure 1

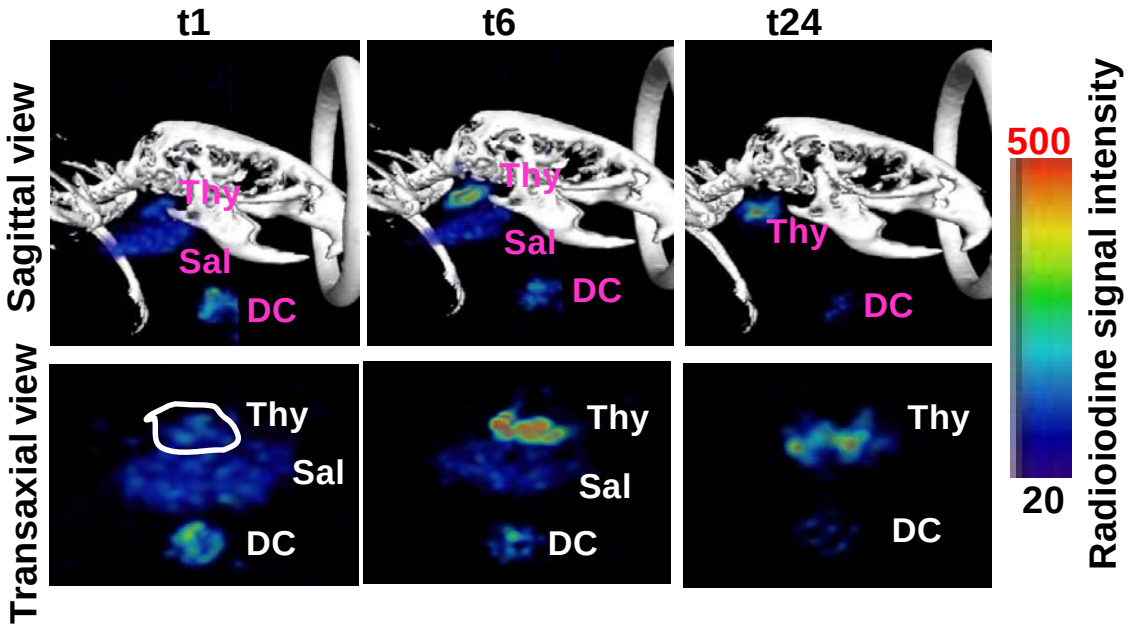
t1
t6
t24
Sagittal view
Transaxial view
Thy
Sal
DC
500
20
Radioiodine signal intensity

Figure 2

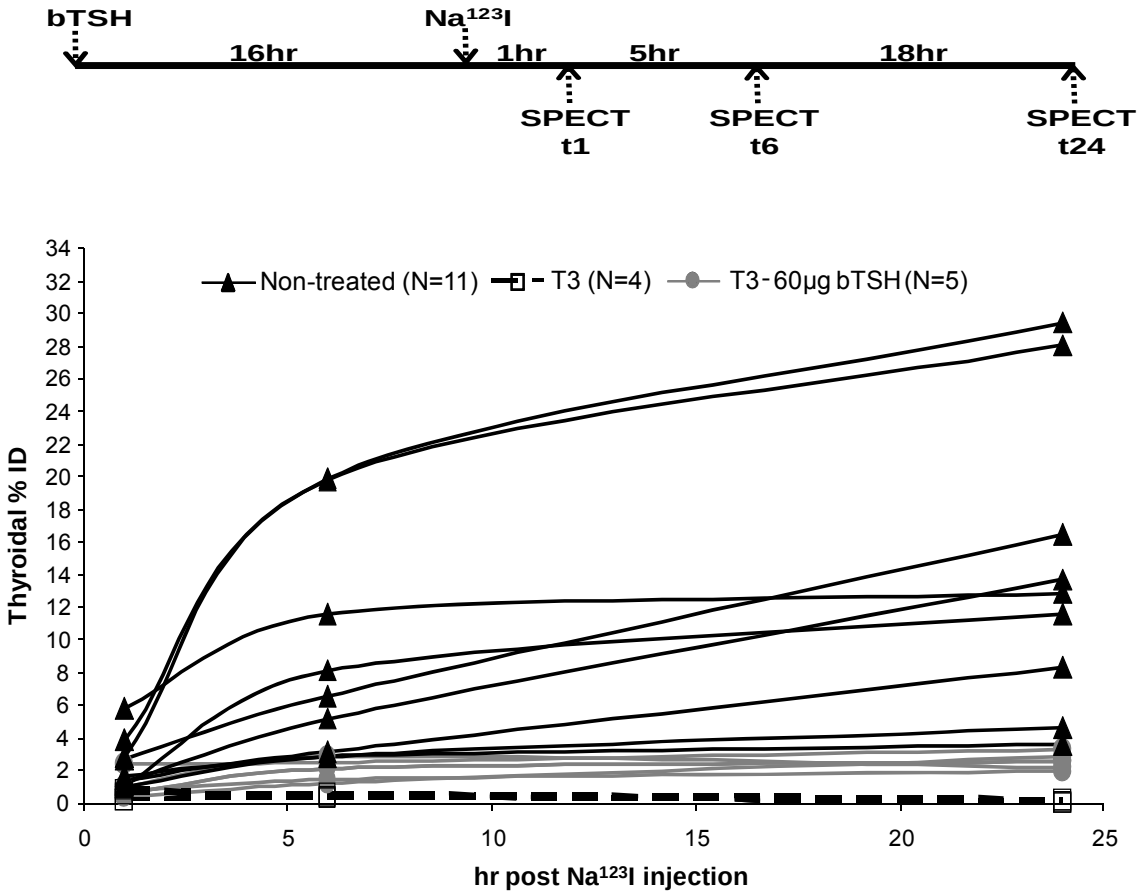
bTSH
Na123I
16hr
1hr
5hr
18hr
SPECT t1
SPECT t6
SPECT t24
Non-treated (N=11)
T3 (N=4)
T3 - 60µg bTSH (N=5)
Thyroidal % ID
hr post Na123I injection

Figure 3

A.

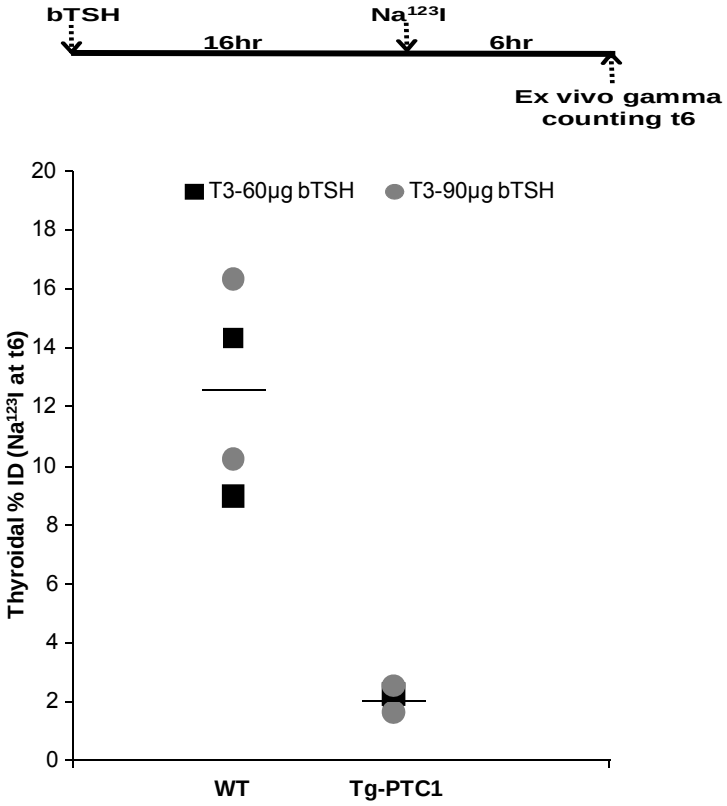
bTSH
16hr
Na123I
6hr
Ex vivo gamma counting t6
T3-60µg bTSH
T3-90µg bTSH
Thyroidal % ID (Na123I at t6)
0
2
4
6
8
10
12
14
16
18
20
WT
Tg-PTC1

B.

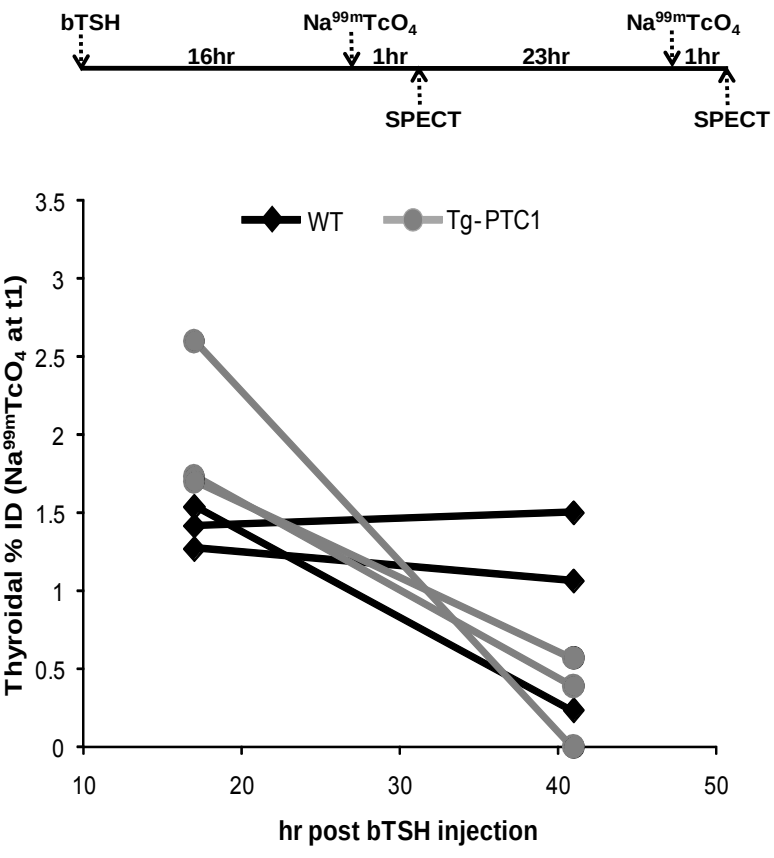
bTSH
16hr
Na99mTcO4
1hr
SPECT
23hr
Na99mTcO4
1hr
SPECT
WT
Tg-PTC1
Thyroidal % ID (Na99mTcO4 at t1)
0
0.5
1
1.5
2
2.5
3
3.5
10
20
30
40
50
hr post bTSH injection

Figure 4

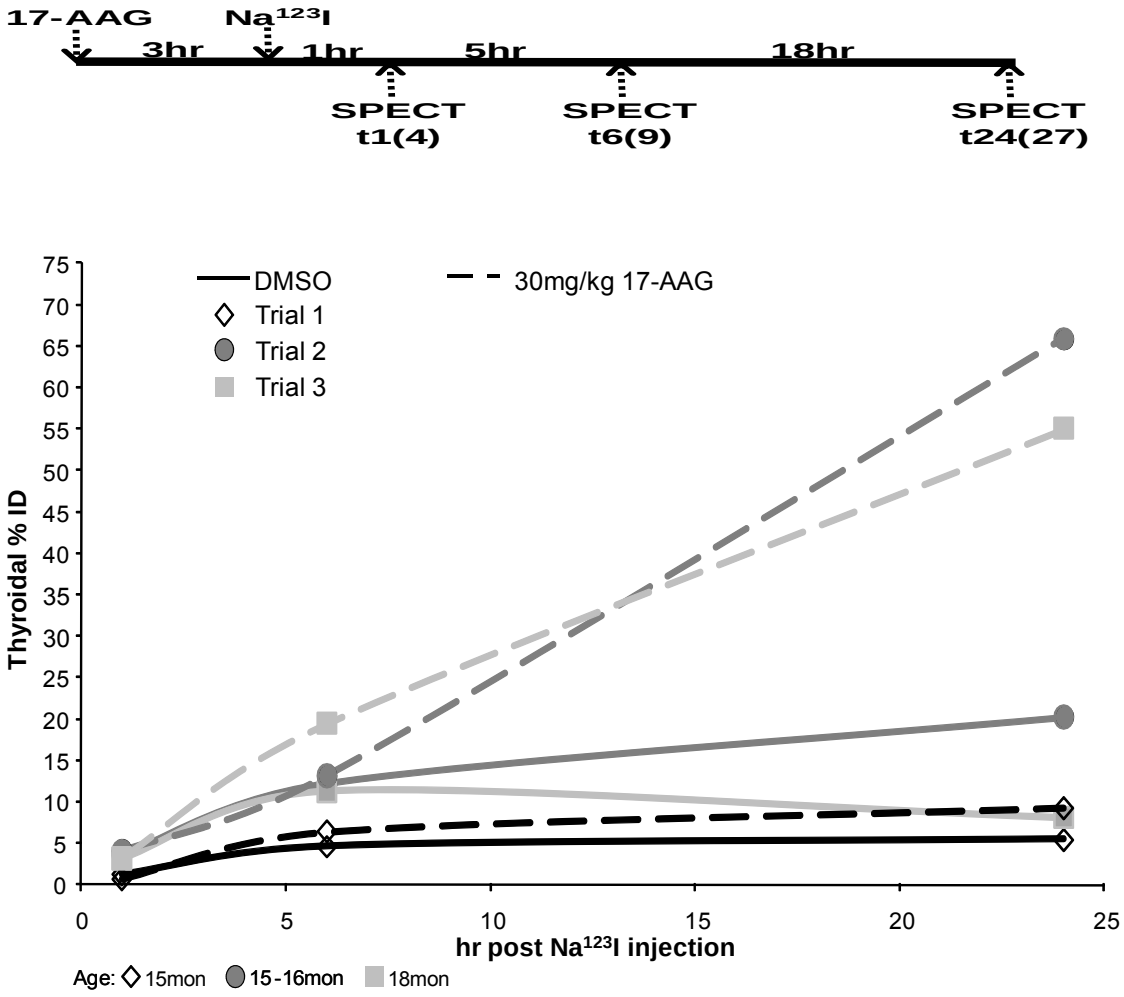
17-AAG
Na123I
3hr
1hr
5hr
18hr
SPECT t1(4)
SPECT t6(9)
SPECT t24(27)
DMSO
30mg/kg 17-AAG
Trial 1
Trial 2
Trial 3
Thyroidal % ID
hr post Na123I injection
Age: 15mon 15-16mon 18mon

Figure 5

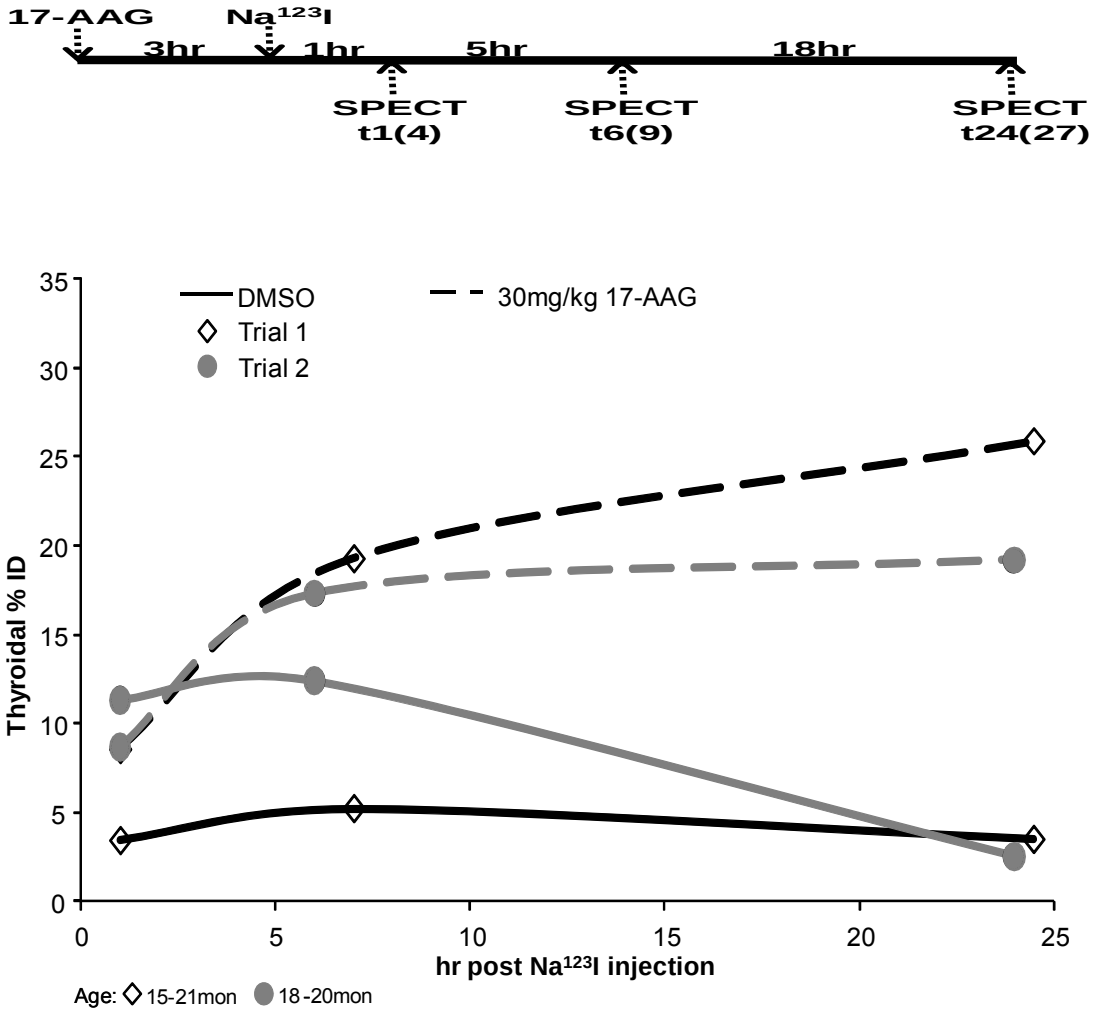
17-AAG
Na123I
3hr
1hr
5hr
18hr
SPECT t1(4)
SPECT t6(9)
SPECT t24(27)
DMSO
30mg/kg 17-AAG
Trial 1
Trial 2
Thyroidal % ID
hr post Na123I injection
Age: 15-21mon 18-20mon

Table 1. Temporal dynamics of thyroidal and salivary radioiodine accumulation in non-treated wild type mice

					Thyroidal iodide				Salivary iodide
		Thyroidal %ID			retention ability		Salivary %ID		retention ability
Gender	Age (mon)	t1	t6	t24	t6/t1	t24/t1	t1	t6	t6/t1
M	2	1.49	2.88	3.62	1.94	2.43	2.74	0.83	0.30
M	3	1.64	3.15	8.30	1.93	5.07	6.47	1.7	0.26
M	7	2.94	18.45	21.26	6.27	7.22	13.62	9.92	0.73
M	14	0.90	5.29	13.06	5.88	14.52	4.59	3.94	0.86
M	15	1.12	8.14	11.60	7.25	10.33	6.46	6.54	1.01
F	3	6.45	12.74	10.46	1.98	1.62	6.57	0.69	0.10
F	4	0.63	1.59	1.48	2.51	2.34	0.93	1.37	1.48
F	6	2.14	23.21	24.66	10.85	11.52	4.89	4.13	0.84

Table 2. Effect of 17-AAG on thyroidal radioiodine accumulation in wild type and Tg-TPC1 mice

Mice	Treatment	Thyroidal % ID			Iodide retention ability		
		t1	t6	t24	6hr/1hr	24hr/1hr	AUC*
WT	DMSO	2.6 ± 1.3	9.3 ± 4.1	11.2 ± 7.9	3.6 ± 0.2	4.3 ± 1.6	224.4 ± 133.2
	17-AAG	2.7 ± 1.8	13.0 ± 6.6	43.4 ± 30.1	6.3 ± 3.4	15.7 ± 0.9	583.1 ± 362.1
Tg-PTC1	DMSO	7.4 ± 5.6	8.8 ± 5.1	3.0 ± 0.7	1.3 ± 0.3	0.6 ± 0.6	148.8 ± 44.3
	17-AAG	9.2 ± 1.0	16.7 ± 2.9	22.6 ± 4.7	1.9 ± 0.5	2.6 ± 0.6	442.6 ± 62.7

*AUC: area under time-activity curve, it is calculated by $\int_{t=24hr}^{t=1hr} f(t)dt$; f(t): thyroidal %ID; d(t): time(hour)